A lock-in-based approach to look through the thermal signatures of magnetic nanoparticles in liquid, solid and aggregated states

Christophe A. Monnier[Λ], Marco Lattuada[Λ], David Burnand[Θ], Federica Crippa[Λ], Julio Cesar Martinez-Garcia [Λ], Ann M. Hirt[Σ], Barbara Rothen-Rutishauser[Λ], Mathias Bonmarin[Ω,*], and Alke Petri-Fink[Λ,Θ,*]

* Corresponding authors: mathias.bonmarin@zhaw.ch, alke.fink@unifr.ch

[Λ] Adolphe Merkle Institute, University of Fribourg, Chemin des Verdiers 4, 1700 Fribourg, Switzerland
[Θ] Chemistry Department, University of Fribourg, Chemin due Musée 9, 1700 Fribourg, Switzerland
[Σ] Institute of Geophysics, ETH Zurich, Sonneggstrasse 5, CH-8092 Zurich, Switzerland
[Ω] Institute of Computational Physics, Zurich University of Applied Sciences, Technikumstrasse 9, 8400 Winterthur, Switzerland

Supplementary Information

The challenges of determining the initial heating slope

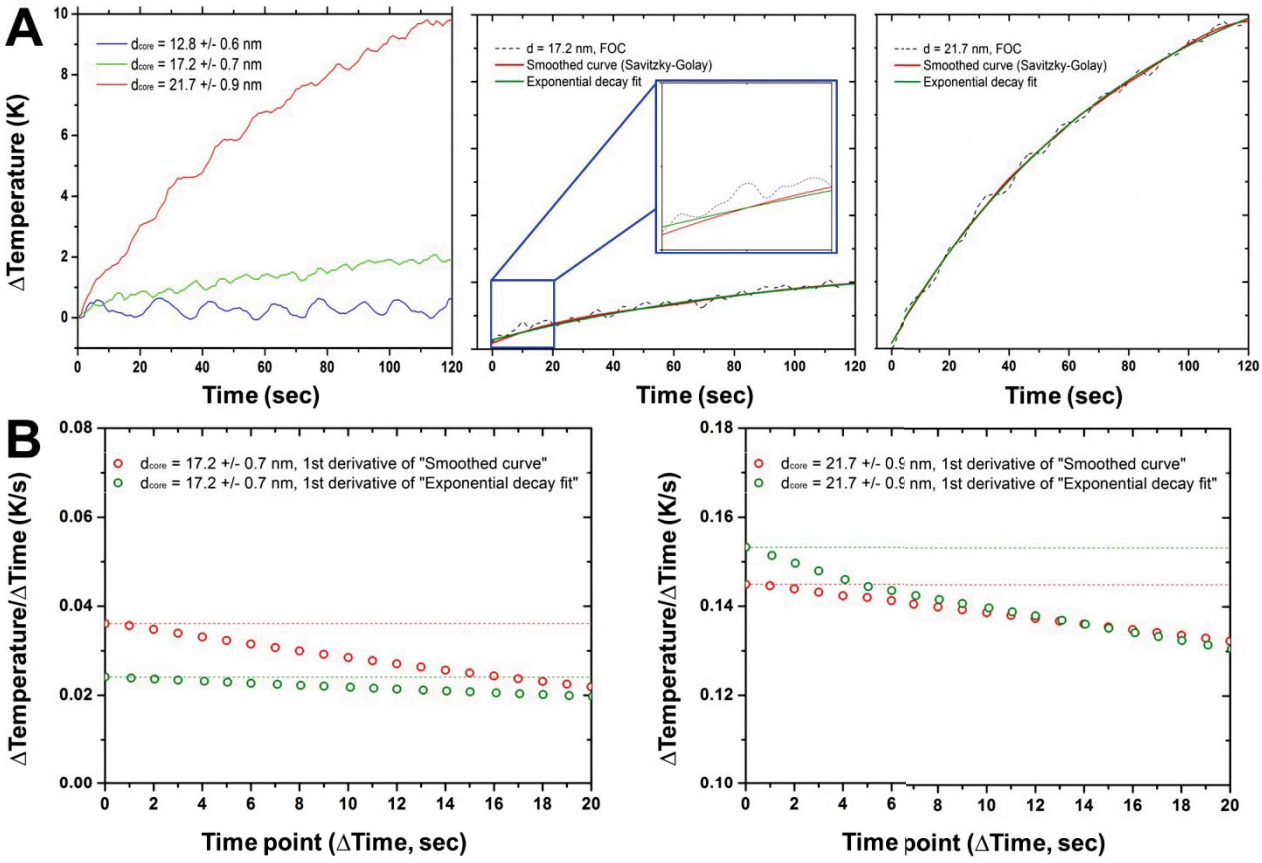

Suppl. Figure 1: Determining the initial heating slope from data recorded under non-adiabatic conditions. The heating behavior of three nanoparticle batches was investigated with fiberoptic cables at 535 kHz/12.5 mT. (A). The data were either smoothed by using the Savitzky-Golay (SG) filtering procedure or fitted with an exponential decay fit. The slope at every time point was then assessed by determining the first derivative of the data points (B).

As highlighted in Suppl. Figure 1, determining the initial heating slope of nanoparticles investigated under non-adiabatic conditions may be delicate. It is strongly influenced by the noise derivative distortion, associated with the experimental error. Depending on the smoothing or fitting procedures, the outcome may vary considerably.

To highlight this fundamental problem, we used the Savitzky-Golay filtering procedure.[1, 2] It is based on the fitting of a subgroup data point array of ($n = 2m+1$ integer with m positive integers from 1 to 12) to a polynomial of degree p ($p \leq 2m$) in the last-squares sense.

$$\frac{\partial}{\partial b_k}\left[\sum_{i=-m}^{i=m}\left(\sum_{k=0}^{n} b_k i^k - y_i\right)^2\right] = 0 \qquad \text{(S.1)}$$

It converts each point of this subgroup to temporary coordinate systems in which the ordinate values range from $i = -m$ to $i = m$, where the midpoint is defined as $i = 0$. All the data within the window is used to perform a least square fit of eq. (S.1), but only the central point is smoothed for each window position. It allows a reduction of the experimental noise keeping its higher moments**.** Consequently, it provides a way for obtaining the resulting functional behaviour of the smoothed and derivatives heating curves, respectively.

The application of the Savitzky-Golay filtering procedure leads to reliable output, even for highly distorted data, as presented in Suppl. Figure 1. The red line represents the curve with s = 0 / smoothed curve, d = 3 / polynomial order, with the filter ($2m+1=15$) points, and seven points on each side. The derivative scatter points were also determined with the same set of parameters.

The lock-in thermography setup

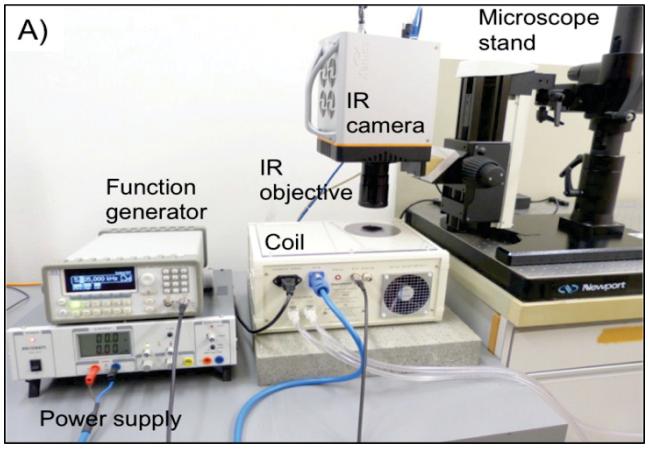

Suppl. Figure 2: An overview of the experimental setup with the various components.

The setup sensitivity σ (K) is theoretically given by

$$\sigma = \frac{NETD}{\sqrt{\frac{N f_{cam}}{f_{mod}}}}$$

NETD represents the noise-equivalent temperature difference of the camera (in K), while f_{cam} is its maximal frequency (Hz). In our case, *NETD* = 0.017 K, f_{cam} = 200 Hz and f_{mod} = 0.5 Hz, giving a sensitivity of 0.00017 K after only 25 modulation cycles (*N*), or 50 seconds of measurement time.

Iron oxide nanoparticles – synthesis details

- **d = 12. 8 ± 0.6 nm**

Iron oleate (7 g):oleic acid (1.465 g), molecular weight ratio = 1.5:1

Boiling solvent: Trioctylamine, 52.4 mL

Heating ramp:

1. 30 – 110 °C: 10 °C/min
2. 110 – 200 °C: 5 °C/min
3. 200 – 320 °C: 3 °C/min

Reflux time: 30 min

- **d = 17. 2 ± 0.7 nm**

Iron oleate (7.23 g):oleic acid (1.0310 g), molecular weight ratio = 2.2:1

Boiling solvent: Trioctylamine, 50.7 mL
Heating ramp:

1. 30 – 170 °C: 10 °C/min
2. 170 – 320 °C: 5 °C/min

Reflux time: 30 min

- **d = 21. 7 ± 0.9 nm**

Iron oleate (7 g):oleic acid (1.220 g), molecular weight ratio = 1.8:1

Boiling solvent: Trioctylamine, 50.7 mL
Heating ramp:

1. 30 – 110 °C: 10 °C/min
2. 110 – 200 °C: 5 °C/min
3. 200 – 320 °C: 3 °C/min

Reflux time: 30 min

- **d = 50. 3 ± 3.6 nm**

Iron oleate (7 g):oleic acid (1.368 g), molecular weight ratio = 1.37:1

Boiling solvent: Docosane, 36.26 mL (solid under 50° C)
Heating ramp:

1. 30 – 110 °C: 10 °C/min
2. 110 – 200 °C: 5 °C/min
3. 200 – 335 °C: 3 °C/min

Reflux time: 60 min

Iron oxide nanoparticles - Characterization

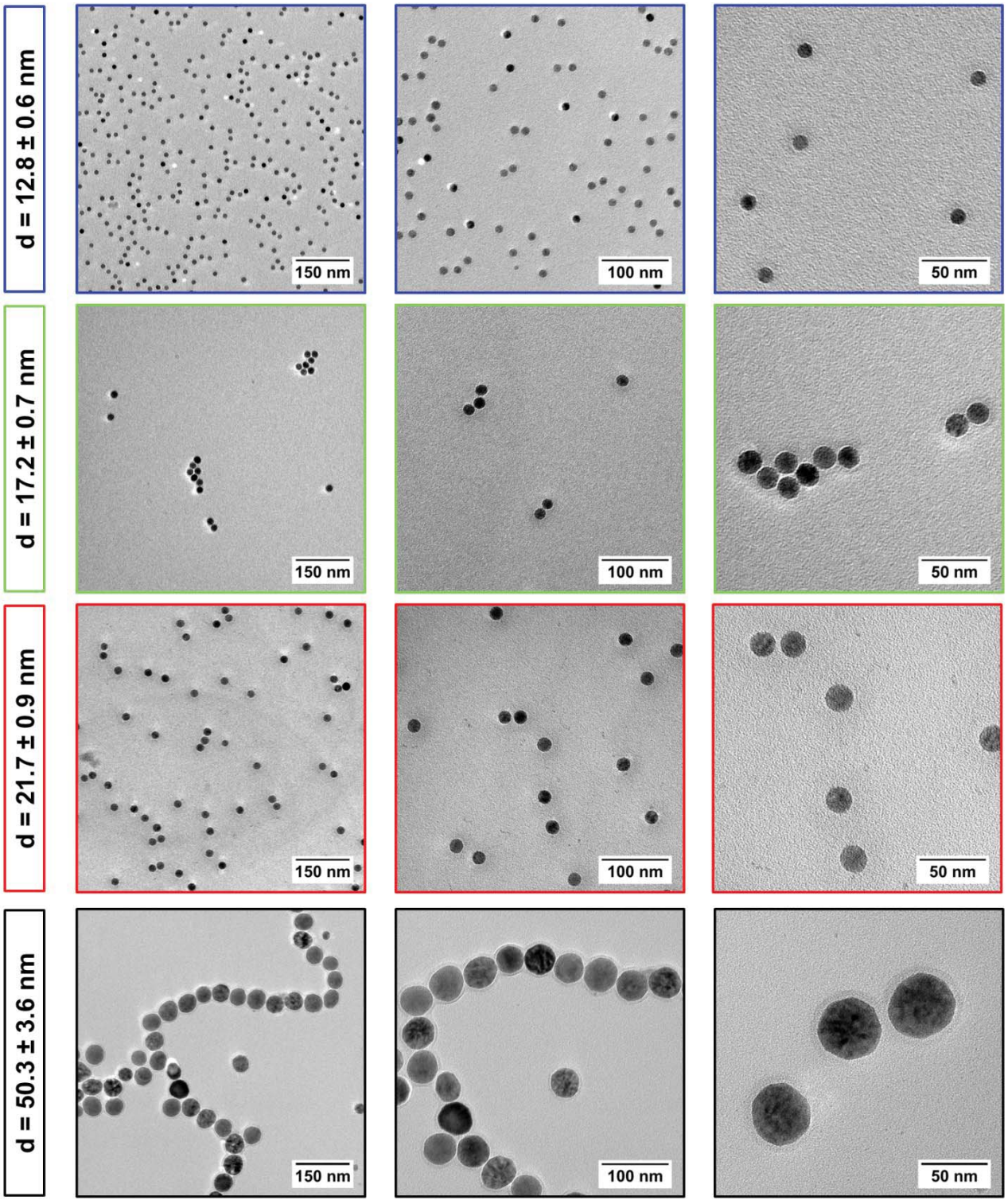

Suppl. Figure 3: All nanoparticles were dried on Cu mesh carbon-coated grids and investigated with a FEI Tecnai transmission electron microscope operating at 200 kV in order to determine the nanoparticle core diameter.

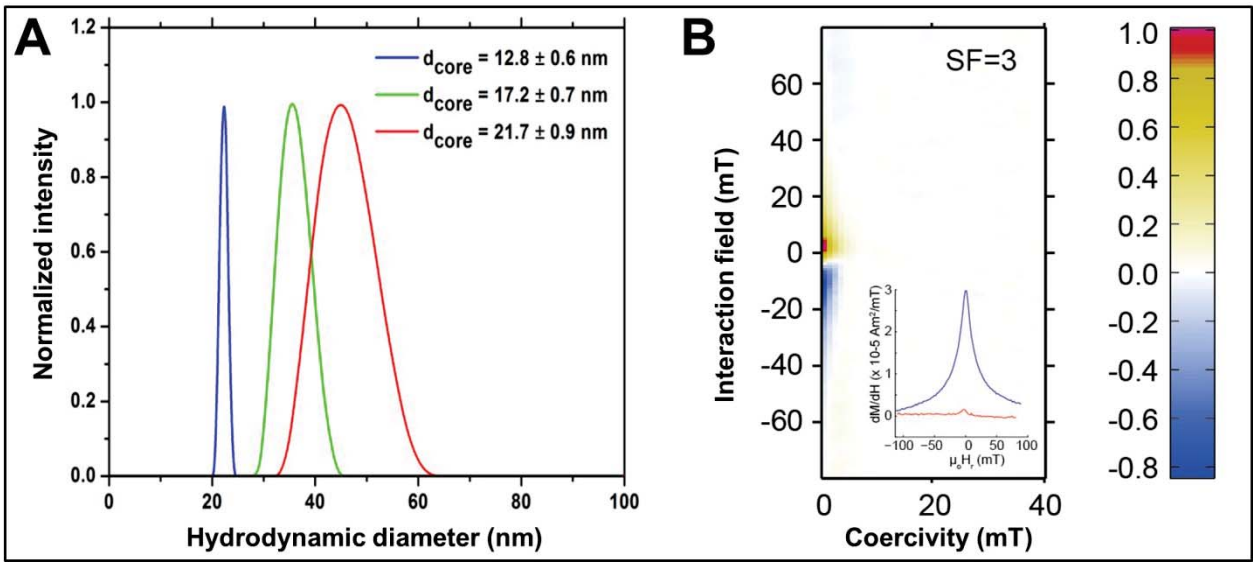

Suppl. Figure 4: The nanoparticles were further investigated by dynamic light scattering to determine their hydrodynamic diameter (A). Nanoparticles with d = 21.7 ± 0.9 nm were additionally investigated by FORC analysis.

Lock-in thermography – Relations between diameters and concentrations

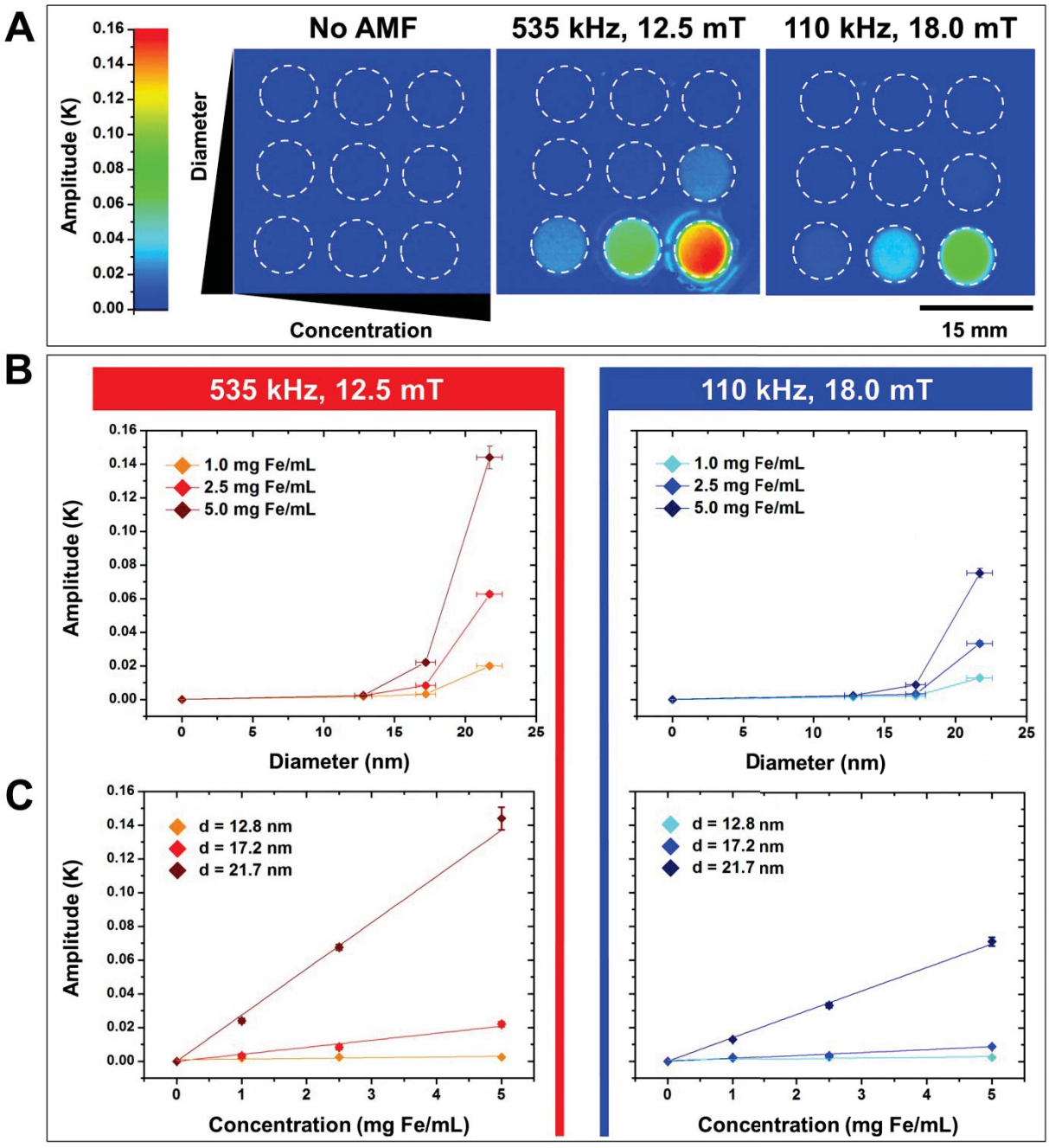

Suppl. Figure 5: Comparative investigations of the nanoparticles at 535 kHz/12.5 mT and 110 kHz/18.0 mT. The iron oxide nanoparticles diluted to three different iron concentrations and simultaneously investigated in regard to their detection capability (A), diameters (B) and concentration (C). The AMF was modulated at a frequency of 0.5 Hz and camera frame rates of 200 Hz. 25 cycles were run.

Standard thermography – Experimental measurements and simulations

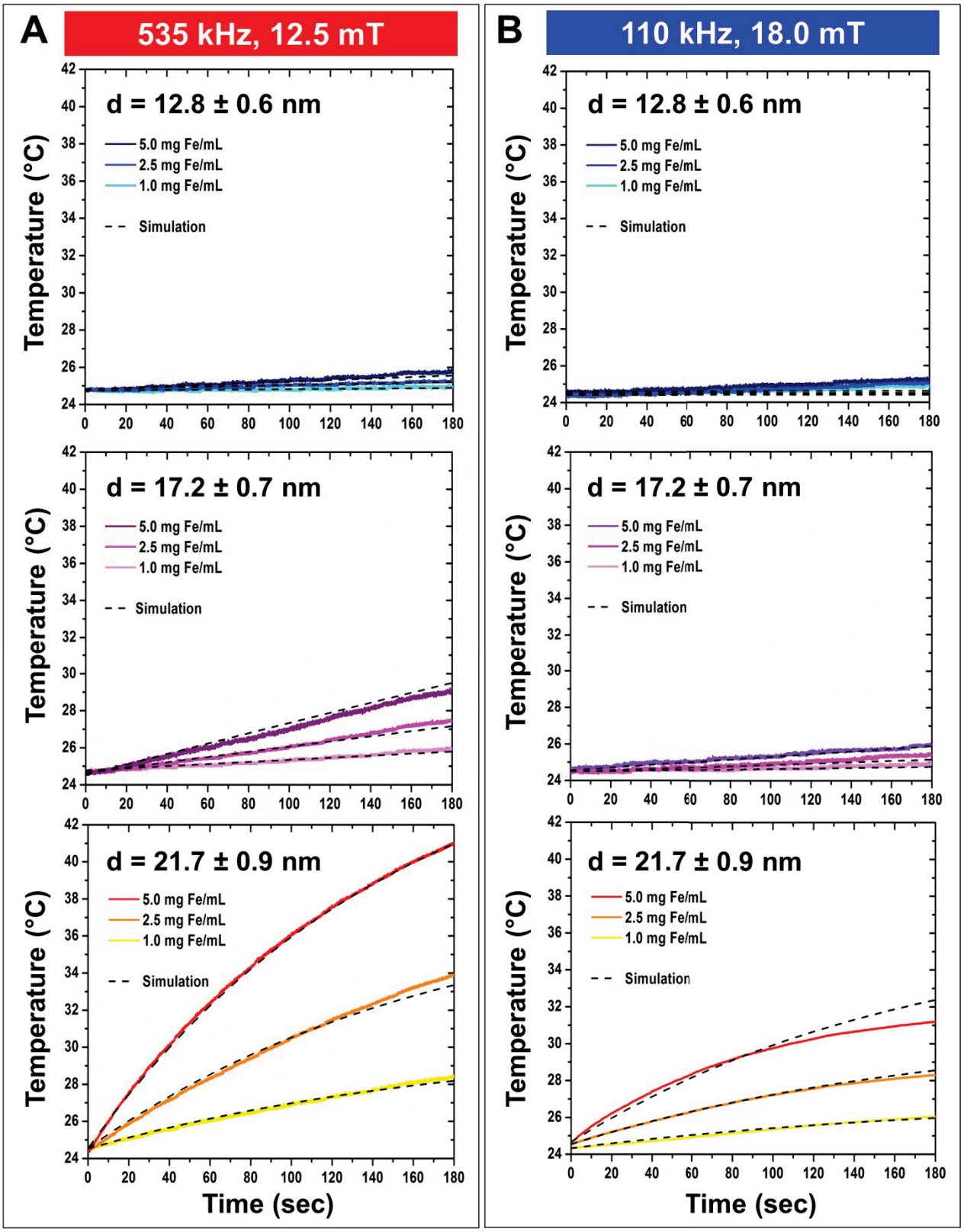

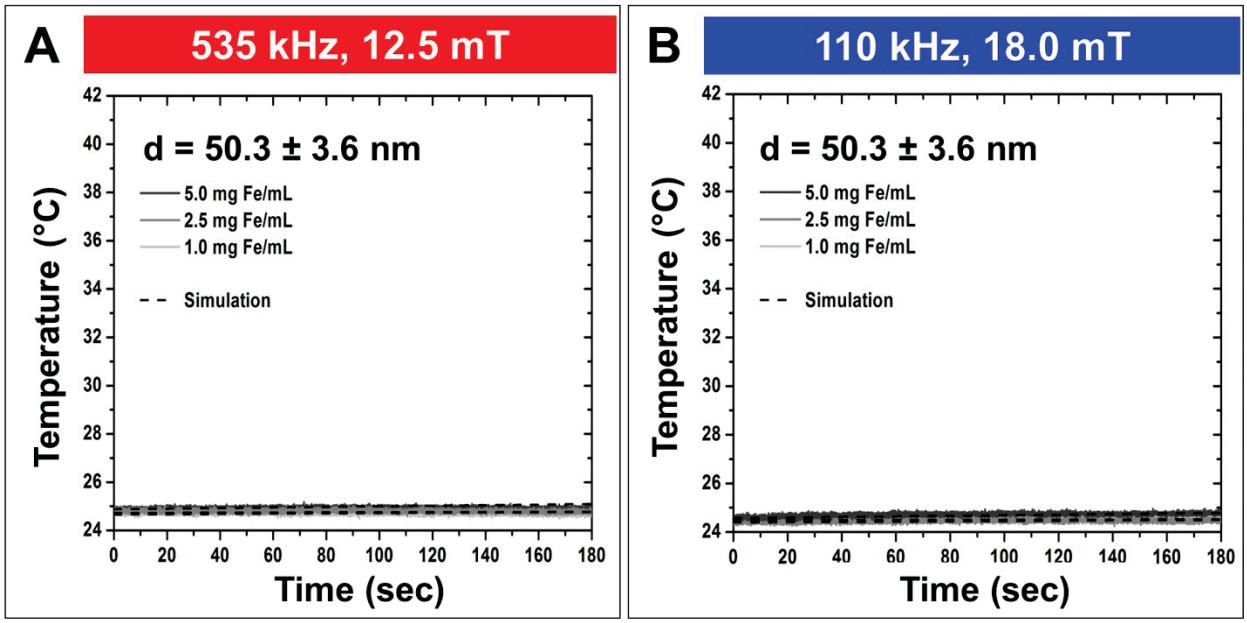

Suppl. Figure 6: The thermal emissions of all nanoparticles at three different iron concentrations were measured over time with magnetic field stenghts and frequencies of (A) 535/12.5 mT and 110 kHz/18.0 mT. The shown measurments were recorded by standard IR thermography. As a reference, the heating curves were simulated (black dashed lines) and compared to the experimental results.

Thermal measurements – Heating slope and ILP values

	Initial slope ß (535 kHz, 12.5 mT), K/s					Initial slope ß (110 kHz, 18.0 mT), K/s			
	d = 12.8 ± 0.6 nm								
	LIT	ST	FOC	SIM		LIT	ST	FOC	SIM
5.0 mg Fe/mL	0.0087	0.0030	0.0023	0.0055		0.0024	0.0028	0.0024	0.0023
2.5 mg Fe/mL	0.0013	0.0056	0.0063	0.0027		0.0016	0.0028	0.0027	0.0011
1.0 mg Fe/mL	0.0016	0.0014	0.0018	0.0011		0.0017	0.0022	0.0015	0.0005
	d = 17.2 ± 0.7 nm								
	LIT	ST	FOC	SIM		LIT	ST	FOC	SIM
5.0 mg Fe/mL	0.0296	0.0250	0.0240	0.0295		0.0078	0.0045	0.0047	0.0086
2.5 mg Fe/mL	0.0131	0.0164	0.0063	0.0146		0.0034	0.0043	0.0027	0.0043
1.0 mg Fe/mL	0.0045	0.0050	0.0034	0.0058		0.0021	0.0024	0.0025	0.0017
	d = 21.7 ± 0.9 nm								
	LIT	ST	FOC	SIM		LIT	ST	FOC	SIM
5.0 mg Fe/mL	0.1460	0.1730	0.1480	0.1599		0.0783	0.0830	0.0860	0.0801
2.5 mg Fe/mL	0.0820	0.0710	0.0863	0.0796		0.0353	0.0297	0.0353	0.0400
1.0 mg Fe/mL	0.0296	0.0259	0.0396	0.0317		0.0149	0.0135	0.0096	0.0160

Suppl. Table 1: A summary of all slope values collected by the various methods. These values were subsequently used to determine the SAR.

	ILP (535 kHz, 12.5 mT), nHm^2/kg Fe					ILP (110 kHz, 18.0 mT), nHm^2/kg Fe			
	d = 12.8 ± 0.6 nm								
	LIT	ST	FOC	SIM		LIT	ST	FOC	SIM
5.0 mg Fe/mL	0.14	0.05	0.04	0.15		0.09	0.10	0.09	0.08
2.5 mg Fe/mL	0.04	0.18	0.05	0.15		0.12	0.21	0.16	0.08
1.0 mg Fe/mL	0.13	0.11	0.14	0.15		0.32	0.41	0.28	0.08
Average	**0.10**	**0.11**	**0.08**	**0.15**		**0.17**	**0.24**	**0.17**	**0.08**
SD	**0.06**	**0.06**	**0.06**	**0.00**		**0.12**	**0.15**	**0.10**	**0.00**
	d = 17.2 ± 0.7 nm								
	LIT	ST	FOC	SIM		LIT	ST	FOC	SIM
5.0 mg Fe/mL	0.47	0.39	0.36	0.41		0.29	0.17	0.17	0.30
2.5 mg Fe/mL	0.41	0.52	0.20	0.41		0.25	0.32	0.20	0.30
1.0 mg Fe/mL	0.35	0.40	0.27	0.41		0.39	0.44	0.46	0.30
Average	**0.41**	**0.44**	**0.28**	**0.41**		**0.31**	**0.31**	**0.28**	**0.30**
SD	**0.06**	**0.07**	**0.08**	**0.00**		**0.07**	**0.14**	**0.16**	**0.00**
	d = 21.7 ± 0.9 nm								
	LIT	ST	FOC	SIM		LIT	ST	FOC	SIM
5.0 mg Fe/mL	2.30	2.72	2.33	2.46		2.78	3.06	3.17	2.63
2.5 mg Fe/mL	2.59	2.24	2.72	2.46		2.47	2.20	2.61	2.63
1.0 mg Fe/mL	2.34	2.05	3.13	2.46		2.77	2.50	1.78	2.63
Average	**2.41**	**2.34**	**2.73**	**2.46**		**2.67**	**2.59**	**2.52**	**2.63**
SD	**0.16**	**0.35**	**0.40**	**0.00**		**0.17**	**0.44**	**0.70**	**0.00**

Suppl. Table 2: All Specific Absorption Rate (SAR) values were converted to Intrinsic Loss of Power (ILP) to provide a more universal reference value.

Polyacrylamide gels – Applied ratios, measurements, simulations and SEM analysis

Gel wt %	AA/Bis 30% (µL)	SPIONs (µL) c = 8.7 mg Fe/mL	MilliQ (µL)	TEMED (µL)	APS 10% (µL)
0.00	332	0	668	1	10
1.00	332	121	547	1	10
2.50	332	302	366	1	10
5.00	332	605	63	1	10

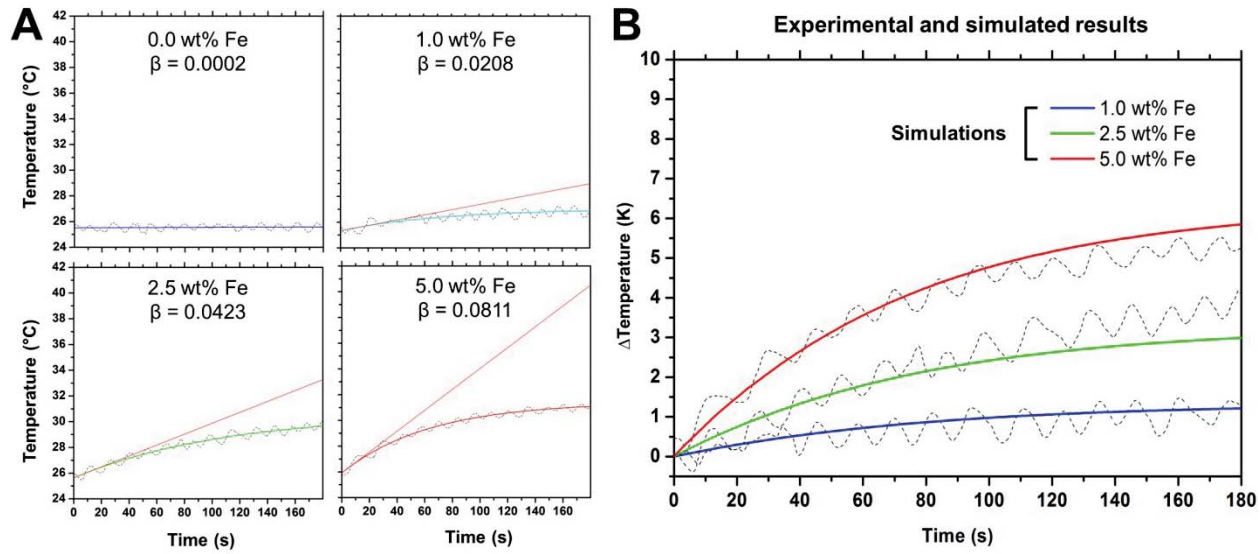

Suppl. Figure 7: Experimental and simulated results from SPION-containing polyacrylamide gels. Polyacrylamide gels containing different SPION concentrations were investigated while being exposed to an AMF with fiberoptic cables (A). The initial heating slopes were determined *via* linear least-square linear fit of the first five measurement seconds. These same parameters were then simulated according to the previously described linear response theory (B) and compared to experimental results.

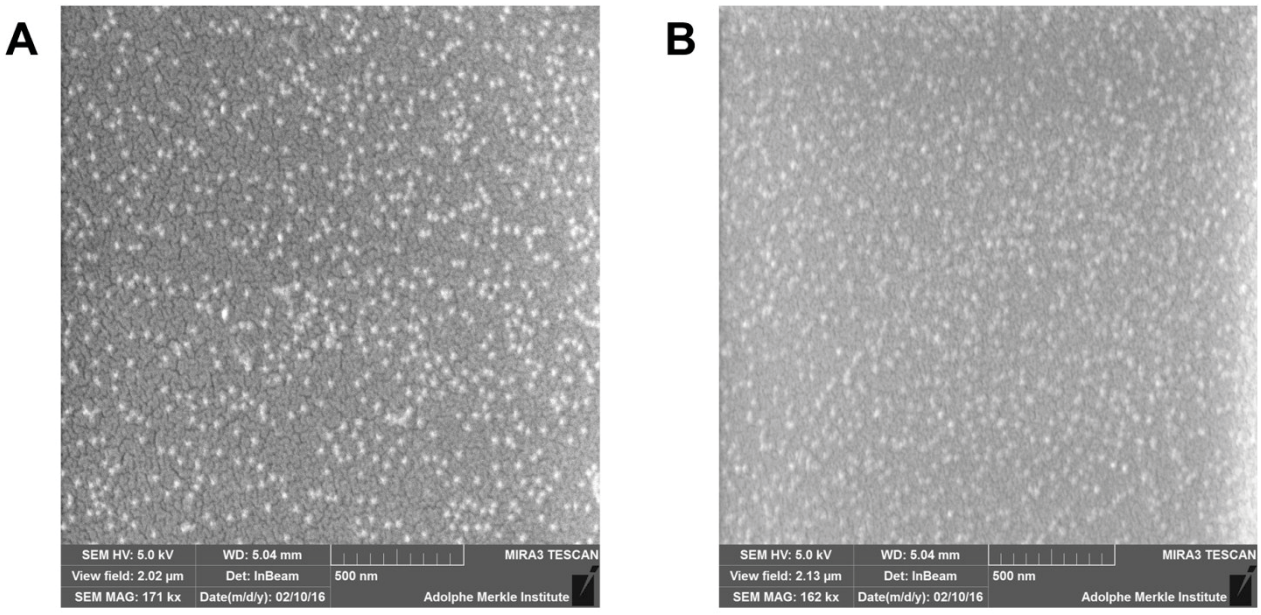

Suppl. Figure 8: SPION distribution in polyacrylamide gels. Scanning electron microscopy images of the respective gels highlighted the homogenous distribution of the magnetic nanoparticles within them.

Mathematical model – Applied values

The following table summarizes the values of parameters used in the simulations.

Particle core diameter (nm)	Saturation magnetization (A/m)	Magnetocrystalline anisotropy constant (535/110 kHz) (J/m^3)	Polymer layer thickness (nm)	τ_0 (s)
12.8	40180	26000/30000	4.7	10^{-9}
17.2	101640	6850/8800	8.9	10^{-9}
21.7	366370	2850/4500	11.55	10^{-9}
50.3	40180	3000/3000	10	10^{-9}

Limitations in thermal resolution

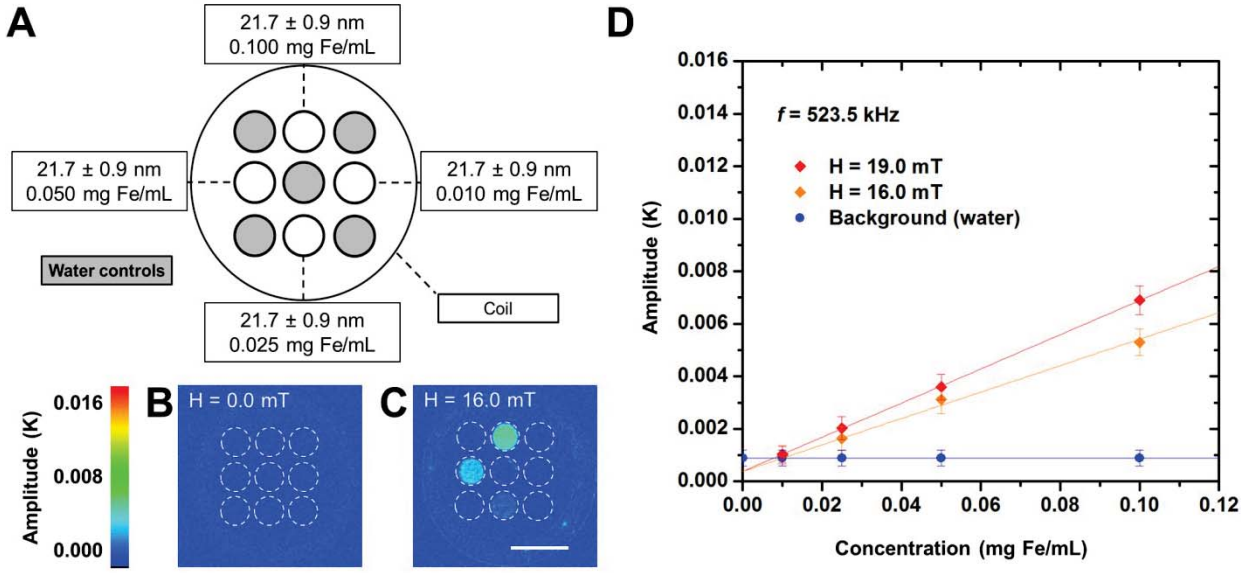

Suppl. Figure 9: Minimum detectable SPION concentrations. SPIONs (d = 21.7 ± 0.9 nm) were diluted down and used to assess the detection limit of the system. Four increasingly dilute suspensions were investigated at 0 mT (*i.e.*, to measure the overall background signal, B), 16.0 mT (C, scale bar = 1 cm) and 19 mT field strength at 200 modulation cycles. The respective signals were then extracted and plotted as a function of NP concentration (D).Concentrations down to 0.025 mg Fe/mL clearly stood out from the background, which represented the overall detection barrier.

References

1. Savitzky, A.; Golay, M. J. Smoothing and differentiation of data by simplified least squares procedures. *Analytical chemistry* 1964, 36, 1627-1639.
2. Martinez-Garcia, J. C.; Martinez-Garcia, J.; Rzoska, S. J.; Hulliger, J. The new insight into dynamic crossover in glass forming liquids from the apparent enthalpy analysis. *The Journal of chemical physics* 2012, 137, 064501.